

THE SURFACE BEHAVIOUR AND CATALYTIC PROPERTIES OF $\text{Nd}_{2-x}\text{Sr}_x\text{CoO}_{4\pm\lambda}$ MIXED OXIDES

Laitao Luo*, Chengwen Liu and Hua Zhong

Department of Chemistry, Nanchang University, Nanchang, 330047, Jiangxi, P.R. China

(Received September 22, 2005; revised December 13, 2005)

ABSTRACT. The mixed oxides, $\text{Nd}_{2-x}\text{Sr}_x\text{CoO}_{4\pm\lambda}$ ($0.4 \leq x \leq 1.2$), (λ = non-stoichiometric oxygen) with the K_2NiF_4 structure were prepared by the polyglycol gel method and used as catalysts for NO reduction. The samples were investigated by IR, TPD, TPR, and XRD methods and iodometry and the effects of the coefficient x on the structure and catalytic activity of the samples were studied. The results show that the $\text{Nd}_{2-x}\text{Sr}_x\text{CoO}_{4\pm\lambda}$ mixed oxides have the K_2NiF_4 structure; other phases are found when $x < 0.4$ and > 1.2 . The amount of Co^{3+} and the lattice oxygen in $\text{Nd}_{2-x}\text{Sr}_x\text{CoO}_{4\pm\lambda}$ increase with increasing x . The catalytic activity of $\text{Nd}_{2-x}\text{Sr}_x\text{CoO}_{4\pm\lambda}$ for NO reduction is closely correlated with the concentration of oxygen vacancies and the amount of Co^{3+} .

KEY WORDS: A_2BO_4 , Co-containing mixed oxide, NO reduction, Rare-earth

INTRODUCTION

The nitrogen oxides (NO) are the most important contaminants in motor vehicle exhaust gases [1-2]. In order to eliminate them, precious metal catalysts are widely used [3-5] but as they are expensive it is necessary to search for low-cost materials. The perovskite-like A_2BO_4 mixed oxides with the K_2NiF_4 structure consisting of alternating layers of ABO_3 , as in perovskite, and AO, as in rock salt, show high catalytic activity and good thermal stability and are also low-cost [6-7]. At present, there are many studies on LnSrCuO_4 and LnSrNiO_4 [8-11], and a few on the oxidation of CO and C_3H_8 on LnSrCoO_4 [12], but no study on NO reduction over LnSrCoO_4 has been reported. This paper describes Co-based mixed oxides $\text{Nd}_{2-x}\text{Sr}_x\text{CoO}_{4\pm\lambda}$ ($0.4 \leq x \leq 1.2$) with the K_2NiF_4 structure and their catalytic activity for the reduction of NO.

EXPERIMENTAL

Preparation of catalysts. A series of oxides $\text{Nd}_{2-x}\text{Sr}_x\text{CoO}_{4\pm\lambda}$ ($x = 0.4-1.2$) were synthesized by the polyglycol gel method. Carefully measured amounts of $\text{Nd}(\text{NO}_3)_3$ ($0.5 \text{ mol}\cdot\text{L}^{-1}$, 32 mL), $\text{Sr}(\text{NO}_3)_2$ ($0.5 \text{ mol}\cdot\text{L}^{-1}$, 8 mL) and citric acid (0.03 mol) were mixed with a solution of $\text{Co}(\text{NO}_3)_2$ ($0.5 \text{ mol}\cdot\text{L}^{-1}$, 20 mL). The volume was reduced to 40 mL at 353 K, then polyglycol 20000 was added and stirring continued until a viscous gel was formed. This was evaporated to dryness, and the residue was calcined at 873 K for 4 h, then pelletized and calcined once more in air at 1373 K for 10 h. The pellet was then pulverized to ca. 0.250~0.177 mm.

Powder X-ray diffraction (XRD) data were obtained by use of a $\text{D}_8/\text{ADVANCE}$ diffractometer. The IR spectra were recorded from KBr pressed disks on a Perkin-Elmer 683 spectrophotometer in the range of $1000-400 \text{ cm}^{-1}$. The average Co valence was determined by iodometry [11].

Temperature programmed desorption (TPD) experiments were carried out with automatic Micromeritics 3000 equipment interfaced to a data station. The samples (0.300 g) were first heated from room temperature to 1123 K at a rate of $8 \text{ K}\cdot\text{min}^{-1}$ in a flow of O_2 ($40 \text{ mL}\cdot\text{min}^{-1}$)

*Corresponding author. E-mail: luolaitao@yahoo.com.cn

and then cooled to room temperature. They were then purged with He for 1 h, and heated from room temperature to 1123 K at the same rate. Temperature programmed reduction (TPR) experiments were carried out in the same apparatus. Since water is produced during reduction, the gases from the reactor were passed through a cold trap before they entered the thermal conductivity detector. The samples (0.100 g) were heated to 1173 K at a rate of 20 K.min⁻¹ in a flow of N₂ (99.9 %) and then cooled to room temperature. They were purged with 10 % H₂/N₂ for 1 h, and then heated to 1173 K at the same rate.

Catalytic activity measurements. NO reduction was studied in a flow reactor by feeding a gas mixture of CO (7.00 vol. %), NO (2.00 % vol. %), and N₂ (91 vol. %) over 0.40 g catalyst, GHSV (gas hour space velocity) = 12000 h⁻¹, at a specific temperature in the range 450-750 K. The gas composition was analyzed before and after the reaction by online gas chromatography with a 5 Å molecular sieve column for NO, N₂ and O₂ and a thermal conductor detector (TCD) connected with a computer integrator system.

RESULTS AND DISCUSSION

Characteristics of solid catalysts

Ganguli [14] proposed that the formation of the K₂NiF₄ structure needs two conditions: a tolerance factor ($t = r_A/r_B$, where r_A and r_B are ionic radii) in the range $1.7 \leq t \leq 2.4$ and electrovalent equilibrium. The XRD patterns of Nd_{2-x}Sr_xCoO₄ mixed oxides ($x = 0.4-1.2$) show that all the Nd_{2-x}Sr_xCoO₄ mixed oxides have the K₂NiF₄ structure (Figure 1). When Nd was substituted by a small amount of Sr ($x = 0.4$) the tolerance factor was close to 1.7; with large amounts of Nd and Co in the sample K₂NiF₄-type mixed oxides are formed, and with a small amounts of Nd and Co formed Nd₂O₃ and CoO. When Nd is substituted by a large amount of Sr ($x = 1.2$), excess Sr cannot enter an A-site because of its larger ionic radius. The formation of SrCO₃ and CoO is confirmed by XRD.

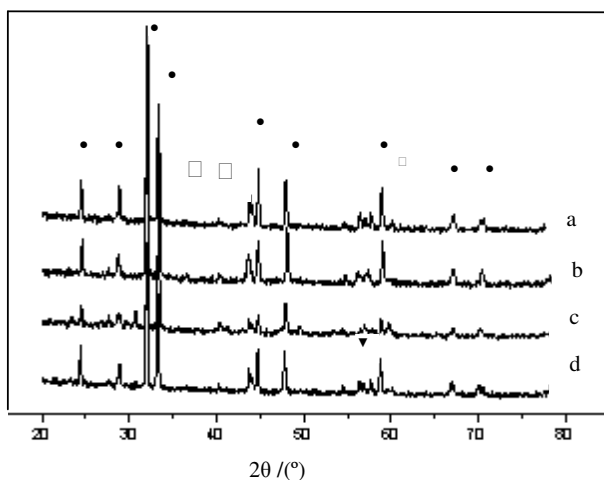


Figure 1. XRD patterns of Nd_{2-x}Sr_xCoO_{4±λ}. a: $x = 0.4$, b: $x = 0.6$, c: $x = 0.8$, d: $x = 1.2$.

•: A₂BO₄ □: Nd₂O₃ ▼: SrCO₃ □: CoO.

The IR spectra of the $\text{Nd}_{2-x}\text{Sr}_x\text{CoO}_{4\pm\lambda}$ mixed oxides are shown in Figure 2. All samples show absorption band around 500 cm^{-1} , characteristic of K_2NiF_4 -type mixed oxides [15]. These results confirm that the series of $\text{Nd}_{2-x}\text{Sr}_x\text{CoO}_{4\pm\lambda}$ mixed oxides have the A_2BO_4 -type structure. The absorption band around 500 cm^{-1} is attributed to the stretching A-O_{II}-B vibration of A_2BO_4 and the absorption band around $650\text{-}680\text{ cm}^{-1}$ is characteristic of C_o-O_x or C_o-O_y bonds in A_2BO_4 structures. The band around $580\text{-}660\text{ cm}^{-1}$ results from the effect of grain size and cannot be attributed to mixed oxides. The band at 850 cm^{-1} belongs to SrCO_3 [16]. These results are confirmed by XRD.

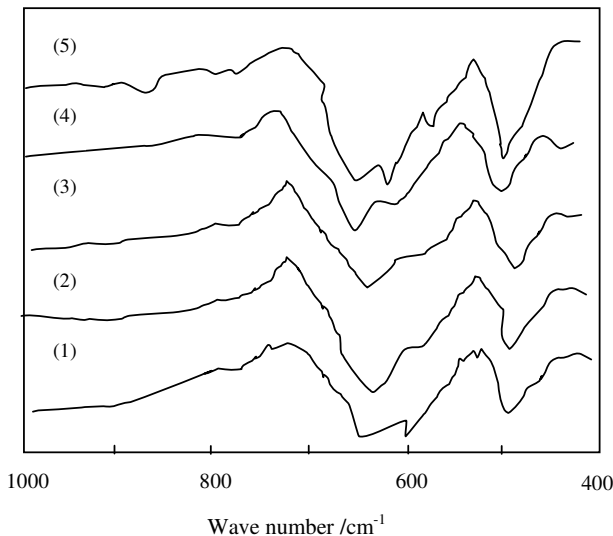
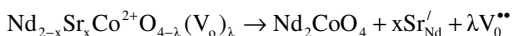
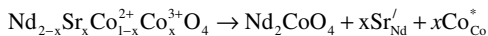


Figure 2. IR patterns of the $\text{Nd}_{2-x}\text{Sr}_x\text{CoO}_{4\pm\lambda}$. (1): $x = 0.4$; (2): $x = 0.6$; (3): $x = 0.8$; (4): $x = 1.0$; (5): $x = 1.2$.

Composition and Co valence of $\text{Nd}_{2-x}\text{Sr}_x\text{CoO}_{4\pm\lambda}$ mixed oxide

In the $\text{Nd}_{2-x}\text{Sr}_x\text{CoO}_{4\pm\lambda}$ mixed oxides ($x = 0.4\text{-}1.2$), when the trivalent ion Nd^{3+} at an A site is replaced by a lower valent Sr^{2+} ion, the reduced positive charge is balanced either by the formation of a higher oxidation state ion at a B-site, i.e. $\text{Co}^{2+} \rightarrow \text{Co}^{3+}$; or by the formation of oxygen vacancy (V_o). These possibilities may exist at the same time, so $\text{Nd}_{2-x}\text{Sr}_x\text{CoO}_{4\pm\lambda}$ has many oxygen vacancies. The processes are shown in the following equations:



where Sr_{Nd}^I is Sr^{2+} at Nd^{3+} and λV_o^{**} is Co^{3+} which has replaced Co^{2+} .

The average Co valence and the Co^{3+} content of the $\text{Nd}_{2-x}\text{Sr}_x\text{CoO}_{4\pm\lambda}$ mixed oxides were determined by iodometric methods and the amounts of non-stoichiometric oxygen (λ) calculated are listed in Table 1. When $0.4 \leq x \leq 1.2$, the average Co valence increases with the increasing x . In addition, the non-stoichiometric oxygen (λ) decreases with increasing x , indicating that the concentration of oxygen vacancies gradually increases.

Table 1. The composition and Co ions valence of $\text{Nd}_{2-x}\text{Sr}_x\text{CoO}_{4\pm\lambda}$ mixed oxide.

| Composition | Average valence | Co^{2+} (%) | Co^{3+} (%) | λ |
|---|-----------------|----------------------|----------------------|-----------|
| $\text{Nd}_{1.6}\text{Sr}_{0.4}\text{CoO}_{4+0.04}$ | 2.4684 | 53.16 | 46.84 | +0.04 |
| $\text{Nd}_{1.4}\text{Sr}_{0.6}\text{CoO}_{4-0.05}$ | 2.4893 | 51.07 | 48.93 | -0.05 |
| $\text{Nd}_{1.2}\text{Sr}_{0.8}\text{CoO}_{4-0.12}$ | 2.5682 | 43.18 | 56.82 | -0.12 |
| $\text{NdSrCoO}_{4-0.20}$ | 2.5821 | 39.79 | 60.21 | -0.20 |
| $\text{Nd}_{0.8}\text{Sr}_{1.2}\text{CoO}_{4-0.28}$ | 2.6452 | 36.48 | 64.52 | -0.28 |

Temperature programmed desorption (O_2 -TPD) of $\text{Nd}_{2-x}\text{Sr}_x\text{CoO}_{4\pm\lambda}$ mixed oxides

The surface oxygen in mixed oxides exists as a series of equilibria: viz O_2 (adsorbed) \leftrightarrow O^- (adsorbed) \leftrightarrow O^- (surface) \leftrightarrow O^{2-} (surface) \leftrightarrow O^{2-} (lattice). The desorption temperature of O^{2-} (lattice) is higher than those of chemisorbed oxygen (O_2 and O^{2-}) [17, 18]. As shown in Figure 3, there are two O^{2-} desorption peaks from $\text{Nd}_{2-x}\text{Sr}_x\text{CoO}_{4\pm\lambda}$ catalysts, one (≤ 600 K) attributed to desorption of the chemisorbed oxygen and the other (≥ 850 K) to loss of lattice oxygen. The amount of chemisorbed oxygen decreases with increasing x , but the amount of lattice oxygen increases, implying that the concentrations of oxygen vacancies and of mobile lattice oxygen also increase. These conclusions confirm those from the iodometric method.

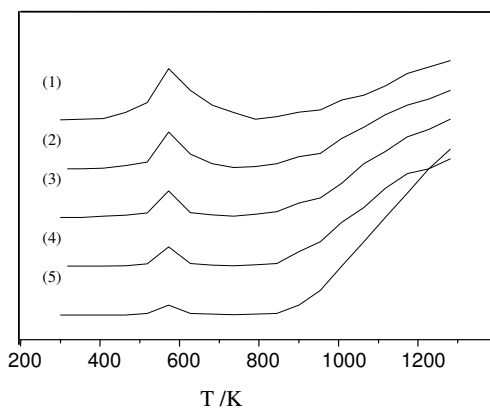
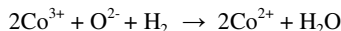


Figure 3. O_2 -TPD profiles over $\text{Nd}_{2-x}\text{Sr}_x\text{CoO}_{4\pm\lambda}$. (1): $x = 0.4$; (2): $x = 0.6$; (3): $x = 0.8$; (4): $x = 1.0$; (5): $x = 1.2$.

Temperature programmed reduction (TPR) of $\text{Nd}_{2-x}\text{Sr}_x\text{CoO}_{4\pm\lambda}$ mixed oxides

As shown in Figure 4, there are two H_2 -reduction peaks over $\text{Nd}_{2-x}\text{Sr}_x\text{CoO}_{4\pm\lambda}$ mixed oxides. The temperature corresponding to the first peak gradually decreases, and the temperature corresponding to the other peak gradually increases with the increasing x . Because Nd^{3+} and Sr^{2+} at A-sites could not be reduced by H_2 under the experimental conditions (400-1200 K), the Co ions at B-sites were reduced by H_2 . The low temperature peak corresponds to the reduction of Co^{3+} and chemisorbed oxygen, and the $\text{Nd}_{2-x}\text{Sr}_x\text{CoO}_{4\pm\lambda}$ catalysts keep their original structure.



The high temperature peak corresponds to the reduction of Co^{2+} ,



with the destruction of the K_2NiF_4 -structure. The temperature corresponding to the second peak increases with the increasing x , implying that the thermal stability of $\text{Nd}_{2-x}\text{Sr}_x\text{CoO}_4$ catalysts increases with increasing x .

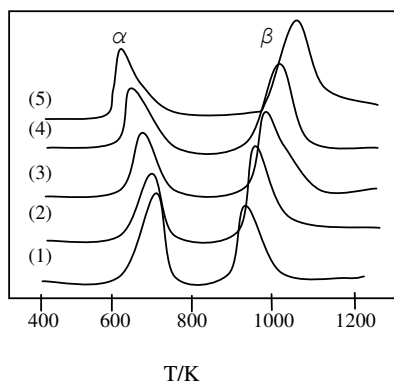
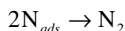
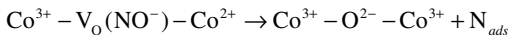
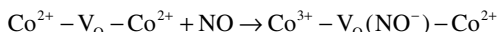
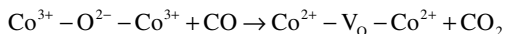


Figure 4. TPR profiles over $\text{Nd}_{2-x}\text{Sr}_x\text{CoO}_{4\pm x}$ catalysts. (1): $x = 0.4$; (2): $x = 0.6$; (3): $x = 0.8$; (4): $x = 1.0$; (5): $x = 1.2$.

Catalytic activity of $\text{Nd}_{2-x}\text{Sr}_x\text{CoO}_{4\pm x}$ mixed oxides for NO reduction

The catalytic activity of $\text{Nd}_{2-x}\text{Sr}_x\text{CoO}_{4\pm x}$ mixed oxides for NO reduction by CO increased with the increase of x , as shown in Figure 5. The mechanism of the reaction between NO and CO over $\text{Nd}_{2-x}\text{Sr}_x\text{CoO}_4$ mixed oxides could be illustrated as follows [19]:



The Co^{3+} in the $\text{Nd}_{2-x}\text{Sr}_x\text{CoO}_4$ mixed oxides plays an important role in the NO reduction, as it is necessary for the regeneration of oxygen vacancies. Co^{3+} can be reduced to Co^{2+} under the reaction conditions, with formation of oxygen vacancies, while Co^{2+} is oxidised to Co^{3+} to regenerate oxygen vacancies and active sites. An increase in the concentration of Co^{3+} and oxygen vacancies is favorable for the reduction of NO.

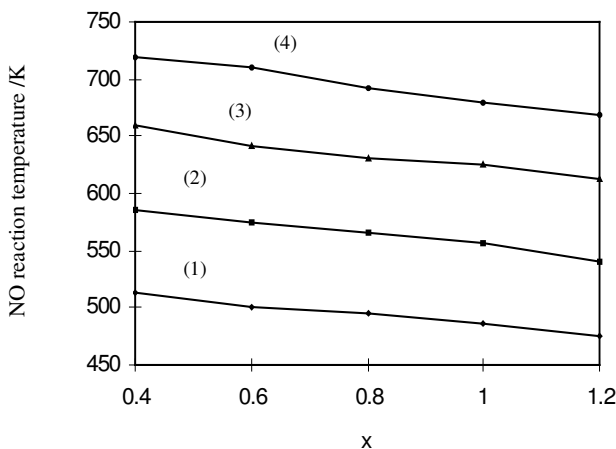


Figure 5. Effects of x to the activities of NO reduction over $\text{Nd}_{2-x}\text{Sr}_x\text{CoO}_{4\pm\lambda}$. NO conversion (%): (1): 100 %, (2): 80 %, (3): 50 %, (4): 20%.

CONCLUSIONS

XRD and IR show the $\text{Nd}_{2-x}\text{Sr}_x\text{CoO}_{4\pm\lambda}$ ($x = 0.4-1.2$) mixed oxides prepared by the polyglycol method have the K_2NiF_6 structure. The amount of Co^{3+} , the non-stoichiometric oxygen (λ) and catalytic activity for NO reduction over $\text{Nd}_{2-x}\text{Sr}_x\text{CoO}_{4\pm\lambda}$ increase with increasing x . It has been found that the catalytic activity for NO reduction is closely correlated with the concentration of oxygen vacancies and of Co^{3+} .

REFERENCES

1. Botas, J.; Gutierrez, O.; Miquel, A. *Appl. Catal. B* **2001**, *32*, 243.
2. Courtois, X.; Perrichon, V.; Primet, M. *Comp. Rend. Serie. Chem.* **2000**, *3*, 429.
3. Kim, D.H.; Woo, S.I.; Noh, J.; Yang, O.B. *Appl. Catal. A* **2001**, *69*, 207.
4. Kobayashi, T.; Yamada, T.; Kayano, K. *Appl. Catal. B* **2001**, *30*, 287.
5. He, H.; Dai, H.X.; Ng, L.H.; Wong, K.W.; Au, C.T. *J. Catal.* **2002**, *1*, 206.
6. Guilhaume, N.; Peter, S.D.; Primet, M. *Appl. Catal. B* **1996**, *10*, 325.
7. Peter, S.D.; Garbowski, E.; Guilhaume, N.; Perrichon, V.; Primet, M. *Catal. Lett.* **1998**, *54*, 79.
8. Ladavos, A.K.; Pomonis, P. *J. Appl. Catal. A* **1998**, *165*, 73.
9. Zhao, Z.; Yang, X.; Wu, Y. *Appl. Catal. B* **1996**, *8*, 281.
10. Gao, L.Z.; Au, C.T. *Catal. Lett* **2001**, *65*, 91.
11. Zhao, Z.; Yang, X.; Wu, Y. *Sci. China Ser. B* **1997**, *40*, 464.
12. Yang, X.M.; Luo, L.T.; Zhong, H. *Appl. Catal. A* **2004**, *272*, 299.
13. Zhang, J.J.; Yang, X.G.; Bi, J.H. *Catal. Today* **1992**, *13*, 555.
14. Gangluli, D. *J. Solid State Chem.* **1979**, *30*, 353.
15. Ogita, N.; Udagawa, M.; Kojima, K. *J. Phys. Soc. Japan* **1988**, *57*, 3982.
16. Zhang, J.J.; Yang, X.G.; Bi, J.H. *Catal. Today* **1992**, *13*, 555.
17. Zhao, Z.; Yang, X.; Liu, Y.; Wu, Y. *J. Science China* **1996**, *41*, 149.
18. Shang, G.; Ge, X.; Zhang, H. *Huaxue Xuebao* **1999**, *15*, 568.
19. Zhao, Z.; Yang, X.; Wang, X.; Wu, Y. *Chem. J. Chin. Univ.* **1996**, *17*, 790.